Analytic vortices and magnetic resonances in rotating superfluid ^{3}He-A

Kazumi Maki
Department of Physics, University of Southern California, Los Angeles, California 90089-0484
(Received 28 October 1982)

We study theoretically three types of analytic vortices in rotating superfluid ^{3}He-A. We have shown that in the Ginzburg-Landau regime and in an axial magnetic field the circular and the hyperbolic vortices form a stable two-dimensional lattice. We study also the spin-wave spectra associated with these three types of vortices. We find that the radial vortex gives rise to the transverse satellite resonance consistent with a recent NMR experiment in rotating ^{3}He-A by Hakonen *et al.* However, the absence of other satellite resonances is quite puzzling.

I. INTRODUCTION

As is well known the condensate of superfluid ^{3}He-A is described in terms of the axial state (i.e., the Anderson-Brinkman-Morel state), which involves both the spin and orbital degrees of freedom. Unlike superfluid ^{4}He, it is known that the superfluid ^{3}He-A supports analytic vortices[1-4] with a soft core, when superfluid ^{3}He-A is rotated and when the rotation speed is not too large. However, until recently there has been no experimental evidence for analytic vortices in the rotating superfluid ^{3}He-A. This situation appears to be completely changed by a recent nuclear magnetic resonance experiment by Hakonen *et al.*[5,6] in rotating superfluid ^{3}He-A in a coaxial magnetic field. Hakonen *et al.*[6] observed a new transverse satellite resonance when superfluid ^{3}He-A is rotated. As we shall see, the observed satellite frequency is consistent with the spin-wave mode associated with a radial (analytic) vortex in a strong magnetic field. Furthermore, the intensity of this satellite resonance is found to increase linearly with the rotation speed Ω. Therefore, we believe that the satellite resonance observed by Hakonen *et al.*[6] provides the first evidence for analytic vortices in ^{3}He-A.

The object of this paper is to study theoretically the spin-wave spectrum associated with analytic vortices. For simplicity we shall limit ourselves to the Ginzburg-Landau regime. Furthermore, we shall consider the case where a strong magnetic field is applied parallel to the axis of rotation of superfluid ^{3}He. In this situation, the $\hat{d}$ vector describing the spin degrees of freedom of the condensate lies almost in the x-y plane, which is perpendicular to the rotation axis, except possibly near the centers of vortices. In this situation the spatial configuration of $\hat{d}$ in rotating ^{3}He-A is mapped to the spatial distribution of disgyrations.[7] Indeed one can fill the two-dimensional space with a regular array of disgyrations with $n=1$ (radial or circular) and $n=1$ (hyperbolic), so that the sum of the indices n over all disgyrations is zero.[7] Far away from the center of each vortex, $\hat{l}$, the orbital vector, is parallel to $\hat{d}$ to minimize the dipole energy. Therefore, in the presence of a strong magnetic field we have three types of 2π analytic vortices[4,8]: the radial, the circular, and the hyperbolic vortex as shown in Fig. 1. Then the two-dimensional vortex lattice can be constructed by the radial and the hyperbolic vortices or by the circular and the hyperbolic vortices as shown in Fig. 2. We shall analyze the spin-wave modes associated with these three types of vortices separately. As mentioned already the magnetic resonance frequency associated with the radial vortex is consistent with the experiment, while those with other vortices have much larger dipole shifts.

According to Fujita *et al.*,[4] the vortex configuration with the lowest free energy involves the circular vortex rather than the radial vortex at least in the Ginzburg-Landau regime. This situation is unaltered even in the presence of a high magnetic field. Therefore, why the radial vortices rather than the other vortices are observed by Hakonen *et al.* is somewhat puzzling. On the other hand, in the low-temperature region, we can show that the radial vortex is more stable than the circular vortex (see the Appendix). Therefore, it is possible that at the actual temperature where the nuclear magnetic resonance experiment is carried out the radial vortex is already more stable than the circular vortex.

More disturbing is the fact that there appears to be no signal from the hyperbolic vortices. According to our present analysis, the hyperbolic vortices should exist in all temperatures in order to complete the vortex lattice. However, the satellite frequency associated with the hyperbolic vortex is quite close to the bulk resonance frequency and therefore it will

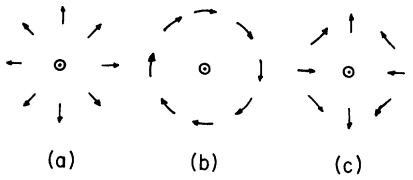

FIG. 1. Three types of analytic vortices are shown: (a) the radial vortex, (b) circular vortex, and (c) the hyperbolic vortex. The arrows indicate the direction of $\hat{l}$. $\odot$ means that $\hat{l}$ is directed upward.

be more difficult to detect. Clearly more accurate determination of the NMR spectrum is desirable.

II. THREE TYPES OF ANALYTIC VORTICES

The order parameter of ^{3}He-A is described by $A_{\mu\nu}$,

$$A_{\mu\nu}=(\Delta_0/\sqrt{2})\hat{\Delta}_\mu d_\nu \ , \tag{1}$$

where the indices μ and ν refer to the orbital and the spin degrees of freedom, respectively. In the Ginzburg-Landau regime and in the presence of a magnetic field in the z direction the free energy is given by[9]

$$F=F_{\rm kin}+E_D+E_H \ ,$$

where

$$\begin{aligned}F_{\rm kin}=\tfrac{1}{2}K\int d^3r[3\,|\,\vec{\nabla}\cdot\vec{\Delta}\,|^2+|\,\vec{\nabla}\times\vec{\Delta}\,|^2 \\ +2\,|\,(\vec{\Delta}\cdot\vec{\nabla})\hat{d}\,|^2 \\ +|\,\vec{\Delta}\,|^2(|\,\vec{\nabla}\cdot\hat{d}\,|^2+|\,\vec{\nabla}\times\hat{d}\,|^2)] \ ,\end{aligned} \tag{2}$$

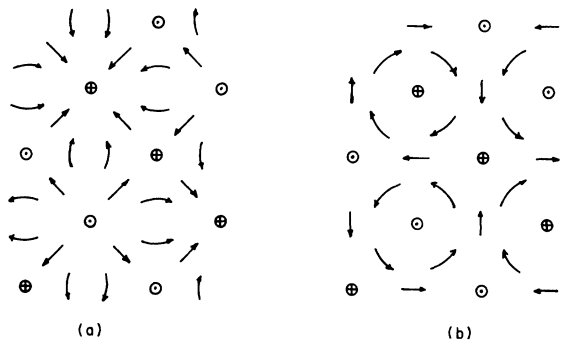

FIG. 2. Two possible vortex lattices are shown: (a) the radial-hyperbolic vortex lattice, and (b) the circular-hyperbolic vortex lattice. The arrows indicate the direction of $\hat{l}$. $\odot$ means that $\hat{l}$ is directed upward while $\oplus$ means the downward direction.

where in the weak-coupling theory K is given by[10]

$$K=\frac{6}{5}\frac{N}{8m^*}\frac{7\zeta(3)}{(2\pi T)^2}$$

and E_D and E_H are the dipole energy and the magnetic energy.

In the presence of a strong magnetic field in the z direction, we can parametrize $\hat{d}$ and $\hat{\Delta}$,

$$\begin{aligned}\hat{d}&=(-\cos\psi\hat{x}+\sin\psi\hat{y})\sin\chi+\cos\chi\hat{z} \ , \\ \hat{\Delta}&=e^{i\alpha}[\cos\beta(\cos\gamma\hat{x}-\sin\gamma\hat{y})+\sin\beta\hat{z} \\ &\quad +i(\sin\gamma\hat{x}+\cos\gamma\hat{y})] \ ,\end{aligned} \tag{3}$$

we find the free energy for a single vortex per unit length f,

$$\begin{aligned}f=\frac{A}{2}\int d^2r([2(\vec{\nabla}\alpha)+\cos\beta(\vec{\nabla}\gamma)]^2+3(\vec{\nabla}\gamma)^2-2\sin^2\beta[(\cos\gamma\alpha_x-\sin\gamma\alpha_y)^2+(\sin\gamma\gamma_x+\cos\gamma\gamma_y)^2] \\ +(\vec{\nabla}\beta)^2+2\sin^2\beta(\cos\gamma\beta_x-\sin\gamma\beta_y)^2 \\ +2\sin\beta\{\beta_x(\alpha_y+\cos\beta\gamma_y)-\beta_y(\alpha_x+\cos\beta\gamma_x) \\ +2(\cos\gamma\beta_x-\sin\gamma\beta_y)[\sin\gamma(\alpha_x+\cos\beta\gamma_x)+\cos\gamma(\alpha_y+\cos\beta\gamma_y)]\} \\ +2\{(1+\cos^2\beta)\,|\,\vec{\nabla}\chi\,|^2+\sin^2\beta(\sin\gamma\chi_x+\cos\gamma\chi_y)^2 \\ +\sin^2\chi[(1+\cos^2\beta)\,|\,\vec{\nabla}\psi\,|^2+\sin^2\beta(\sin\gamma\psi_x+\cos\gamma\psi_y)^2]\} \\ +4\xi_\perp^{-2}\{1-[\cos\chi\cos\beta+\sin\chi\sin\beta\cos(\gamma-\psi)]^2\}+4\xi_H^{-2}\cos^2\chi) \ ,\end{aligned} \tag{4}$$

where we assumed that α, β, γ, χ, and ψ are independent of z. Here $\xi_\perp$ and ξ_H are the dipolar coherence length ($\xi_\perp=C_\perp/\Omega_A\sim 10$ μm) and the magnetic coherence length [$\xi_H=(H_0/H)\xi_\perp$, where $H_0=27$ Oe]. In the experiment of Hakonen *et al.*[5,6] with $H=284$ Oe, we obtain $\xi_H\simeq 10^{-1}\xi_\perp$.

We are interested in an isolated vortex configuration not only because it is the simplest case to be analyzed

but also because the vortex density is quite low in the actual experimental setup. Furthermore, we shall confine ourselves to the solutions with axial symmetry in the case of the radial-circular vortex, while in the case of the hyperbolic vortex we shall allow small axial asymmetry. We shall consider, in the following, two separate cases.

A. Radial-circular vortex

The radial and circular vortices belong to a family of solutions given by

$$\alpha=\phi, \quad \psi=\gamma=-\phi+\gamma_0 , \tag{5}$$

where ϕ is the azimuthal angle and γ_0 is a constant; $\gamma_0=0$ corresponds to the radial vortex while $\gamma_0=\pi/2$ to the circular vortex. Furthermore, β and χ depend only on r the radial distance. Then Eq. (4) reduces to

$$f=\pi A\int_0^{r_0} r\,dr\left[\frac{1}{r^2}[5-8\cos\beta+3\cos^2\beta+2\sin^2\chi(2-\sin^2\gamma_0\sin^2\beta)]\right.$$

$$\left.+(1+2\cos^2\gamma_0\sin^2\beta)\beta_r^2+2(2-\cos^2\gamma_0\sin^2\beta)\chi_r^2+4\xi_\perp^{-2}\sin^2(\chi-\beta)+4\xi_H^{-2}\cos^2\chi\right] , \tag{6}$$

where $A=\frac{1}{2}K\Delta_0^2$ and r_0 is the radius of an effective circle occupied by a single vortex line; r_0 can be expressed in terms of the vortex density n_v or the rotation speed Ω as

$$r_0=(\pi n_v)^{-1/2}=(K/2\pi\Omega)^{1/2} , \tag{7}$$

where $K=h/(2m)=0.661\times10^{-3}$ cm^2/sec.

We shall determine β and χ variationally; we assume that $\beta(r)$ and $\chi(r)$ are given by

$$\cos\beta=e^{-(\eta r)^2}, \quad \cos\chi=e^{-(\zeta r)^2} , \tag{8}$$

where η and ζ are the variational parameters. The assumption (8) is consistent with the known behaviors[11] of β and χ; β and χ increase linearly with r from the origin where $\beta=\chi=0$. On the other hand, the approach to $\beta=\chi=\pi/2$ for large r is exponential, which is somewhat slower than the ones described by Eq. (8). Then we find

$$f=\pi A\{(9-2\sin^2\gamma_0)\ln[(\gamma^*)^{1/2}\eta r_0]-4\ln(\eta/\zeta)+(\tfrac{1}{2}-\sin^2\gamma_0)\ln2+\tfrac{5}{12}\pi^2+\cos^2\gamma_0$$

$$+[\sin^2\gamma_0-2\zeta(3)\cos^2\gamma_0](\eta/\zeta)^2+\xi_\perp^{-2}\eta^{-2}+(\xi_H^{-2}-\xi_\perp^{-2})\zeta^{-2}\} , \tag{9}$$

where

$$\gamma^*=1.781\ldots .$$

In Eq. (9) we have kept only the lowest-order terms in $(\eta/\zeta)^2$ as $\eta/\zeta\sim10^{-1}$. Minimizing Eq. (9) with η and ζ, we obtain

$$\eta^2=2\xi_\perp^{-2}\left[5-2\sin^2\gamma_0+8\left[\frac{\sin^2\gamma_0-2\zeta(3)\cos^2\gamma_0}{5-2\sin^2\gamma_0}\right]p\right]^{-1} , \tag{10}$$

$$\zeta^2=\tfrac{1}{2}\xi_H^{-2}\left[1-\left[1+2\frac{(\sin^2\gamma_0-2\zeta(3)\cos^2\gamma_0)}{5-2\sin^2\gamma_0}\right]p\right] , \tag{11}$$

where $p=(\xi_H/\xi_\perp)^2$. Finally the free energy of a single vortex is given by

$$f=\pi A\left[(9-2\sin^2\gamma_0)\ln\left[\frac{(\gamma^*)^{1/2}r_0}{\xi_\perp}\right]-2\ln p+\tfrac{5}{12}\pi^2+\tfrac{9}{2}+\cos^2\gamma_0\right.$$

$$\left.+2\cos^2\gamma_0\ln2-\tfrac{1}{2}(5-2\sin^2\gamma_0)\ln(5-2\sin^2\gamma_0)+0p\right] . \tag{12}$$

The free energy is minimized when $\gamma_0=\pi/2$, which corresponds to the circular vortex:

$$f_{\rm circ}=\pi A\left[7\ln\left[\frac{(\gamma^*)^{1/2}r_0}{\xi_\perp}\right]-2\ln p+\tfrac{5}{12}\pi^2+\tfrac{7}{2}-\tfrac{3}{2}\ln 3\right]. \tag{13}$$

Similarly for the radial vortex with $\gamma_0=0$, we obtain

$$f_{\rm rad}=\pi A\left[9\ln\left[\frac{(\gamma^*)^{1/2}r_0}{\xi_\perp}\right]-2\ln p+\tfrac{5}{12}\pi^2+\tfrac{11}{2}+2\ln 2-\tfrac{5}{2}\ln 5\right]. \tag{14}$$

Therefore, even in the case of a strong magnetic field where $p\ll 1$, we have

$$f_{\rm rad}>f_{\rm circ} \tag{15}$$

in the Ginzburg-Landau regime. This generalizes the result obtained by Fujita *et al.*[4] However, as we shall see in the Appendix at low temperatures $f_{\rm rad}<f_{\rm circ}$; the radial vortex becomes more stable than the circular vortex. It is of great interest to identify the transition temperature where $f_{\rm rad}=f_{\rm circ}$. Our variational solution for $f_{\rm rad}$ with $\eta^2=\frac{2}{5}\xi_\perp^{-2}$ and $\zeta^2=\frac{1}{2}\xi_H^{-2}$ is compared with a numerical solution by Passvogel *et al.*[11] and we find a good agreement for $r\lesssim\xi_\perp$. For $r>\xi_\perp$ our solution approaches $\beta=\pi/2$ somewhat faster than the numerical solution.

B. Hyperbolic vortex

The hyperbolic vortex[4] is found by assuming that

$$\alpha=\phi,\quad \psi=\gamma=\phi+\gamma_0,$$

It can be easily seen that the vortex energy is independent of γ_0; γ_0 controls the orientation of the vortex in the x-y plane. Therefore, without loss of generality we can take $\gamma_0=0$. Then Eq. (4) reduces to

$$\begin{aligned}f_{\rm hyp}=\tfrac{1}{2}A\int_0^{2\pi}d\phi\int_0^{r_0}r\,dr\Bigg[&\frac{1}{r^2}\{5+8\cos\beta+3\cos^2\beta+2\sin^2\chi[2-\sin^2(2\phi)\sin^2\beta]\}\\&+[1+2\cos^2(2\phi)\sin^2\beta]\beta_r^2+2[2-\cos^2(2\phi)\sin^2\beta]\chi_r^2\\&+4\xi_\perp^{-2}\sin^2(\chi-\beta)+4\xi_H^{-2}\sin^2\chi\Bigg].\end{aligned} \tag{16}$$

Now, again assuming that β and χ are given by

$$\cos\beta=-e^{-(\eta r)^2},\quad \cos\chi=-e^{-(\zeta r)^2}, \tag{17}$$

where we assume that η depends on ϕ as well, we obtain

$$\begin{aligned}f_{\rm hyp}=\tfrac{1}{2}A\int_0^{2\pi}d\phi\Bigg[&[5-2\sin^2(2\phi)]\ln[(\gamma^*)^{1/2}\eta r_0]+4\ln[(2\gamma^*)^{1/2}\zeta r_0]-\frac{3}{2}\ln 2+\frac{5\pi^2}{12}+\cos^2(2\phi)\\&+[\sin^2(2\phi)-2\zeta(3)\cos^2(2\phi)]\left[\frac{\eta}{\zeta}\right]^2+\xi_\perp^{-2}(\eta^{-2}-\zeta^{-2})+\xi_H^{-2}\zeta^{-2}\Bigg].\end{aligned} \tag{18}$$

Minimizing $f_{\rm hyp}$, we obtain

$$\begin{aligned}&\eta^2=2[4+\cos(4\phi)]^{-1}\xi_\perp^{-2},\\&\zeta^2=\tfrac{1}{2}\xi_H^{-2},\end{aligned} \tag{19}$$

and

$$f_{\rm hyp}=\pi A\left[8\ln\left[(\gamma^*)^{1/2}\frac{r_0}{\xi_\perp}\right]-2\ln p+\tfrac{5}{12}\pi^2+\tfrac{9}{2}+\tfrac{1}{2}\ln 2-\{2[\ln(4+\sqrt{15})+\ln\tfrac{1}{2}]+2-\tfrac{1}{2}\sqrt{15}\}\right] . \tag{20}$$

As was already mentioned in Sec. I, in order to form a regular vortex lattice, we need either the circular-hyperbolic vortex pairs or the radial-hyperbolic vortex pairs. The parameters η and ζ characterizing these three vortices are summarized in Table I.

III. MAGNETIC RESONANCES

The spin-wave spectrum in the presence of an inhomogeneous texture is analyzed, by studying a small oscillation of $\hat{d}$ around the equilibrium configuration.[12,13] Parametrizing $\hat{d}$ as

$$\hat{d}=[-\cos(\psi+f)\hat{x}+\sin(\psi+f)\hat{y}]\sin(\chi+g)+\cos(\chi+g)\hat{z} \tag{21}$$

we derive the eigenvalue equations for f and g, where f and g describe the longitudinal mode and the transverse mode, respectively. We shall consider, in the following, two separate cases.

A. Radial-circular vortex

In this case the eigenvalue equations are given by

$$\lambda_f f=-\frac{1}{r}\frac{\partial}{\partial r}[r(1-\tfrac{1}{2}\cos^2\gamma_0\sin^2\beta)f_r]+(1-\cos^2\beta)f \tag{22}$$

and

$$\lambda_g g=-\frac{1}{r}\frac{\partial}{\partial r}[r(1-\tfrac{1}{2}\cos^2\gamma_0\sin^2\beta)g_r]+(1-2\cos^2\beta)g , \tag{23}$$

where γ_0 is the parameter introduced in Eq. (5) and $\cos\beta$ is assumed to be given by Eq. (8). The frequency and the length are written in units of Ω_A and $\xi_\perp$. In deriving Eq. (23), we take into account the fact that $g(r,\phi)$, which couples to the homogeneous rf field has the ϕ dependence of the form[13]

$$g(r,\phi)=g(r)e^{\pm i\phi} . \tag{24}$$

From the eigenvalues of Eqs. (22) and (23), the satellite resonance frequencies are given by

$$\omega_l^{\rm sat}=R_l\Omega_A,\quad \omega_t^{\rm sat}=(\omega_0^2+R_t^2\Omega_A^2)^{1/2} , \tag{25}$$

where $R_l^2=\lambda_f$, $R_t^2=\lambda_g$, and ω_0 is the Larmor frequency.

We have determined variationally the eigenfrequencies λ_f and λ_g for the circular and radial vortices, which are summarized again in Table I.

Furthermore, the intensity of the transverse satellite resonance is obtained from

$$I=2\pi\left|\int_0^\infty r\,dr\,g\right|^2\Big/\int_0^\infty r\,dr\,g^2 , \tag{26}$$

and we find for the circular and the radial vortex

$$I_{\rm cir}=14.8(2\pi\xi_\perp^2),\quad I_{\rm rad}=2.9(2\pi\xi_\perp^2) , \tag{27}$$

respectively.

TABLE I. Size parameters η and ζ and the dipole shift parameters R_t and R_l, which describe the satellite resonance frequencies of three types of analytical vortices are summarized. The radial vortex is most extended in space and as a consequence gives rise to the smallest dipole shifts.

Vortex	$\eta\xi_\perp$	$\zeta\xi_H$	R_t	R_l
Radial	$\sqrt{2/5}$	$\frac{1}{\sqrt{2}}$	0.702	0.943
Circular	$\sqrt{2/3}$	$\frac{1}{\sqrt{2}}$	0.935	0.997
Hyperbolic	$\left[\frac{2}{4+\cos(4\phi)}\right]^{1/2}$	$\frac{1}{\sqrt{2}}$	0.8485	0.988

B. Hyperbolic vortex

In this case the corresponding eigenvalue equations are given by

$$\lambda_f f=-\frac{1}{r}\frac{\partial}{\partial r}[r(1-\tfrac{1}{4}\sin^2\beta)f_r]+(1-\cos^2\beta)f , \tag{28}$$

$$\lambda_g g = -\frac{1}{r}\frac{\partial}{\partial r}[r(1-\tfrac{1}{4}\sin^2\beta)g_r]+(1-2\cos^2\beta)g \ . \tag{29}$$

Here we have neglected ϕ dependence of η for simplicity. Again the eigenvalues for f and g are given in Table I. We have also the related intensity

$$I_{\rm hyp}=6.4(2\pi\xi_1^2) \ . \tag{30}$$

IV. CONCLUDING REMARKS

We have studied the magnetic resonance spectra of three types of analytic vortices in superfluid ^{3}He-A in a strong axial magnetic field. We find that out of the three types of vortices, the observed satellite frequency is consistent with the radial vortex. Furthermore, the intensity of this resonance increases with the rotation speed as

$$I_{\rm total}=\tfrac{1}{2}I_{\rm rad}n_v=2.9(2\pi\xi_1^2)\frac{\Omega}{K}=2.9(\xi_\perp/r_0)^2 \tag{31}$$

in the equilibrium configuration. This linear dependence appears to be also consistent with the experimental observation.

On the other hand, if we limit ourselves to the Ginzburg-Landau regime, the circular vortex is more stable than the radial vortex. Therefore, we believe that a transition from the circular vortex to the radial vortex should take place slightly below the superfluid transition temperature, since we know at low temperatures the radial vortex is more stable. Another puzzling aspect is that there seems to be no indication of the existence of the hyperbolic vortex. However, since the related satellite frequency is so close to the bulk resonance, it is possible that the satellite resonance associated with the hyperbolic vortex may be completely masked by the bulk resonance.

After completing this work, I received a report by Seppälä and Volovik.[14] They analyzed the satellite frequencies of the singular and analytic vortices and concluded that the experimental observation is consistent with existence of analytic vortices. However, they studied only the case of the 4π vortex rather than the 2π vortex studied in this paper.

ACKNOWLEDGMENTS

I would like to thank Dr. Hakonen *et al.* for sending me their experimental results prior to publication. I am also grateful to Professor L. Tewordt and Dr. G. Volovik for sending me their work prior to publication. This work was supported by the National Science Foundation under Grant No. DMR-79-16703.

APPENDIX: VORTEX FREE ENERGIES AT LOWER TEMPERATURES

The free-energy function which is valid for all temperatures is obtained by Cross,[15] and can be written as

$$\begin{aligned} f=\tfrac{1}{2}\chi_N C_\perp^2\int d^2r\{&K_1(\hat{l}\cdot\vec{\nabla}\Phi)^2+K_2(\hat{l}\times\vec{\nabla}\Phi)^2+K_3(\vec{\nabla}\Phi)\cdot[\text{curl}\,\hat{l}-\hat{l}(\hat{l}\cdot\text{curl}\,\hat{l})]\\ &-K_4(\vec{\nabla}\Phi)\cdot\hat{l}(\hat{l}\cdot\text{curl}\,\hat{l})+K_5(\text{div}\,\hat{l})^2+K_6(\hat{l}\times\text{curl}\,\hat{l})^2+K_7(\hat{l}\cdot\text{curl}\,\hat{l})^2\\ &+|(\hat{l}\times\vec{\nabla})\hat{d}|^2+\lambda|(\hat{l}\cdot\vec{\nabla})\hat{d}|^2+\xi_\perp^{-2}[1-(\hat{l}\cdot\hat{d})^2]+\xi_H^{-2}\hat{d}_z^2\} \ , \end{aligned} \tag{A1}$$

where

$$\begin{aligned} &K_1=\rho_{S\parallel}/\rho_{S\perp}^{\rm spin},\quad K_2=\rho_{S\perp}/\rho_{S\perp}^{\rm spin},\quad K_3=K_2(\rho_{S\parallel}^0/\rho_{S\perp}^0),\quad K_4=K_1,\quad K_5=\tfrac{1}{4}(1+\tfrac{1}{3}F_1)^{-1}\rho_{S\perp}^0/\rho_{S\perp}^{\rm spin} \ ,\\ &K_6=(1+\tfrac{1}{3}F_1)^{-1}\left[\tfrac{1}{2}\rho_{S\parallel}^0+\frac{1}{12}\frac{F_1}{1+\frac{1}{3}F_1(\rho_{n\perp}^0/\rho)}\rho_{S\parallel}^0\left[\frac{\rho_{S\parallel}^0}{\rho}\right]+\tfrac{2}{3}\tilde{\gamma}\rho\right]\Big/\rho_{S\perp}^{\rm spin} \ ,\\ &K_7=\tfrac{1}{3}(1+\tfrac{1}{3}F_1)^{-1}\left[\tfrac{1}{4}\rho_{S\perp}^0+\rho_{S\parallel}^0+\frac{1}{4}\frac{F_1}{1+\frac{1}{3}F_1(\rho_{n\parallel}^0/\rho)}(\rho_{S\parallel}^0)^2/\rho\right]\Big/\rho_{S\perp}^{\rm spin} \ ,\\ &\lambda=\rho_{S\parallel}^{\rm spin}/\rho_{S\perp}^{\rm spin},\quad \chi_N C_\perp^2=(\hbar^2/2m)^2\rho_{S\perp}^{\rm spin} \ , \end{aligned} \tag{A2}$$

and ρ_{Si}, $\rho_{Si}^{\rm spin}$, and ρ_{Si}^0 are the mass, the spin, and the irreducible superfluid density, and $\tilde{\gamma}$ is another quantity introduced by Cross,[15]

$$\tilde{\gamma}=3\int\frac{d\Omega}{4\pi}\frac{\hat{p}_3^4}{1-\hat{p}_3^2}\phi(\hat{p})$$

and

$$\phi(\hat{p})=1-\frac{\beta}{2}\int_0^\infty d\xi\,\mathrm{sech}^2[\tfrac{1}{2}\beta E(\hat{p})]$$

with

$$E(\hat{p})=[\xi^2+\Delta^2(1-\hat{p}_3^2)]^{1/2}\,. \tag{A3}$$

The free energy for analytic vortices are obtained as in Sec. II. However, it is necessary to identify Φ by

$$\vec{\nabla}\Phi=\vec{\nabla}\alpha+\cos\beta\vec{\nabla}\gamma \tag{A4}$$

and $\hat{l}$ is given by

$$\hat{l}=(-\cos\gamma\hat{x}+\sin\gamma\hat{y})\sin\beta+\cos\beta\hat{z}\,. \tag{A5}$$

Then, making use of the same variation functions for β and χ, we obtain for the radial-circular vortex,

$$f=\pi\chi_N C_1^2\{[(K_1+K_6+\lambda-1)\sin^2\gamma_0+(K_2+K_5)\cos^2\gamma_0]\ln[(\gamma^*)^{1/2}\eta r_0]+\ln[(\gamma^*)^{1/2}\zeta r_0]$$
$$+\tfrac{1}{12}\pi^2(\cos^2\gamma_0 K_5+\sin^2\gamma_0 K_7+1)-\tfrac{1}{2}\cos^2\gamma_0(K_5-K_6)+\tfrac{1}{4}[\xi_\perp^{-2}\eta^{-2}+(\xi_H^{-2}-\xi_\perp^{-2})\zeta^{-2}]\}\,. \tag{A6}$$

By minimizing f for η and ζ, we obtain

$$\eta^2=\xi_\perp^{-2}[2K(\gamma_0)]^{-1}\,,$$
$$\zeta^2=\tfrac{1}{2}(\xi_H^{-2}-\xi_\perp^{-2})\,, \tag{A7}$$

with

$$K(\gamma_0)=(K_1+K_6+\lambda-1)\sin^2\gamma_0+(K_2+K_5)\cos^2\gamma_0\,. \tag{A8}$$

From this it is easy to see that the radial vortex becomes more stable than the circular vortex when

$$K(0)<K\left[\frac{\pi}{2}\right]\,. \tag{A9}$$

In the vicinity of the Ginzburg-Landau regime K_i's are expanded in powers of $\epsilon=1-T/T_c$ as

$$K_1=\tfrac{1}{2}+\tfrac{1}{3}(\tfrac{1}{2}A_1-B_1)\epsilon\,,$$
$$K_2=1+\tfrac{2}{3}(A_1-B_1)\epsilon\,,$$
$$K_5=\tfrac{1}{4}-\tfrac{1}{6}B_1\epsilon\,, \tag{A10}$$
$$K_6=\tfrac{3}{4}+\tfrac{1}{2}(\tfrac{1}{3}A_1-B_1)\epsilon\,,$$
$$\lambda=\tfrac{1}{2}-\tfrac{1}{6}B_1\epsilon\,,$$

where

$$A_1=F_1/(1+\tfrac{1}{3}F_1)$$

and

$$B_1=F_1^a/(1+\tfrac{1}{3}F_1^a) \tag{A11}$$

and F_1 and F_1^a are the Fermi-liquid coefficients. Substituting (A10) into (A8), we obtain

$$K(0)=\tfrac{5}{4}+(\tfrac{2}{3}A_1-\tfrac{5}{6}B_1)\epsilon$$

and

$$K\left[\frac{\pi}{2}\right]=\tfrac{3}{4}+(\tfrac{1}{3}A_1-B_1)\epsilon\,. \tag{A12}$$

Then making use of F_1 and F_1^a at the melting pressure[16,17] $F_1=15.66$ and $F_1^a=-1.33$ we obtain

$$K(0)\cong\tfrac{5}{4}+3.67\epsilon,\quad K\left[\frac{\pi}{2}\right]\cong\tfrac{3}{4}+3.23\epsilon\,. \tag{A13}$$

Therefore, within the present approximation, the circular vortex is more stable than the radial vortex.

On the other hand, in the low-temperature regime we have

$$K_1=K_2=K_3=K_4=(3+F_1)/(3+F_1^a)\,,$$
$$K_5=\tfrac{1}{4}(1+\tfrac{1}{3}F_1^a)^{-1}\,, \tag{A14}$$
$$K_6=K_5\left[2+\tfrac{1}{3}F_1+8\ln\left[\frac{2T_c}{T}\right]-\frac{32}{3}\right],\quad \lambda=1\,.$$

Substituting this, we obtain

$$K(0)=(1+\tfrac{1}{3}F_1^a)^{-1}(\tfrac{5}{4}+\tfrac{1}{3}F_1)$$

and

$$K\left[\frac{\pi}{2}\right]=(1+\tfrac{1}{3}F_1^a)^{-1}\left[\tfrac{5}{12}F_1-\tfrac{7}{6}+2\ln\left[\frac{2T_c}{T}\right]\right] \tag{A15}$$

which implies that $K(\pi/2)>K(0)$ in the low-temperature region. Therefore, at low temperatures the radial vortex becomes more stable than the circular vortex.

[1]N. D. Mermin and T. L. Ho, Phys. Rev. Lett. 36, 594 (1976).

[2]P. W. Anderson and G. Toulouse, Phys. Rev. Lett. 38, 508 (1977).

[3]G. E. Volovik and N. B. Kopnin, Zh. Eksp. Teor. Fiz. Pis'ma Red. 25, 26 (1977) [JETP Lett. 25, 22 (1977)].

[4]T. Fujita, M. Nakahara, T. Ohmi, and T. Tsuneto, Prog. Theor. Phys. 60, 671 (1978).

[5]P. J. Hakonen, O. T. Ikkala, S. T. Islander, O. V. Lounasmaa, T. K. Markkula, P. Roubeau, K. M. Soloheimo, E. L. Andronikashvili, D. I. Garibashvili, and J. S. Tsakadze, Phys. Rev. Lett. 48, 1838 (1982).

[6]P. J. Hakonen, O. T. Ikkala, and S. T. Islander, Phys. Rev. Lett. 50, 1258 (1982).

[7]K. Maki, J. Low Temp. Phys. 32, 1 (1978).

[8]M. Nakahara, T. Ohmi, T. Tsuneto, and T. Fujita, Prog. Theor. Phys. 62, 874 (1979).

[9]P. G. de Gennes, Phys. Lett. 44A, 271 (1973).

[10]V. Ambegaokar, P. G. de Gennes, and D. Rainer, Phys. Rev. A 9, 2676 (1974).

[11]T. Passvogel, N. Schopohl, M. Warnke, and L. Tewordt, J. Low Temp. Phys. 46, 161 (1982); T. Passvogel, N. Schopohl, and L. Tewordt (unpublished).

[12]K. Maki and P. Kumar, Phys. Rev. Lett. 38, 557 (1977); Phys. Rev. B 16, 182 (1977); 17, 1088 (1978).

[13]R. Bruinsma and K. Maki, Phys. Rev. B 18, 1101 (1978).

[14]H. K. Seppälä and G. E. Volovik (unpublished).

[15]M. C. Cross, J. Low Temp. Phys. 21, 525 (1975).

[16]J. C. Wheatley, Rev. Mod. Phys. 47, 415 (1975).

[17]Here we made use of F_1^a, which is deduced from the temperature dependence of R_l associated with the composite soliton (Ref. 12). A similar value of F_1^a is also deduced in D. D. Osheroff, W. van Roosbroeck, H. Smith, and W. F. Brinkman, Phys. Rev. Lett. 38, 134 (1977).